

**PREPARATION AND CHARACTERIZATION OF ZEOLITE Y –  
BASED CATALYST FOR SONOCATALYTIC DEGRADATION  
OF ORGANIC DYES IN WATER**

**ATHEEL HASSAN ALWASH**

**UNIVERSITI SAINS MALAYSIA**

**2013**

**PREPARATION AND CHARACTERIZATION OF ZEOLITE Y –  
BASED CATALYST FOR SONOCATALYTIC DEGRADATION  
OF ORGANIC DYES IN WATER**

**by**

**ATHEEL HASSAN ALWASH**

**Thesis submitted in fulfillment of the requirements  
for the degree of Doctor of Philosophy**

**April 2013**

## ACKNOWLEDGEMENTS

In the name of God the most gracious the most merciful

Praise be to Allah, Lord of the Worlds

My profound gratitude goes to the Almighty God for his divine purpose. He helped, quickened, sustained and strengthened and made me stable in all the difficult situations throughout the period of my PhD study.

Indeed, I would like to express my sincere gratitude and acknowledgements to my supervisor Assoc. Prof. Dr. Ahmad Zuhairi Abdullah for all the support, inspiration, supervision and encouragement throughout undertaking this research. His dedication and insightful guidance have significantly contributed to successful achievement of this work. Thank you Dr. may the Almighty God bless you abundantly. I am also grateful to my co-supervisor, Dr. Norli Ismail for her support throughout the work.

I sincerely thank the management, most especially the Dean, Prof. Azlina Bt. Harun @ Kamaruddin and all the academic staff and lab assistance of School of Chemical Engineering, Universiti Sains Malaysia for granting me good environment to carry out my research work. Furthermore, I greatly appreciate the Institute of Postgraduate School, Universiti Sains Malaysia for its huge contribution in terms of grant and for granting me Graduate Assistantship during the course of the study. Also I would like to acknowledge my employer, Al-Nahrain University for giving me a space to complete my PhD. study.

I would like to express my heartfelt appreciation and love to my wonderful mother for her great sacrifices and support along my life. Without her encouragement and advice, it would have been a great task to achieve my dream. To the soul of my lovely father, for his support and protection along my life. I hope he will be proud of me if he was among us. Also I acknowledge the support of my brother Mr. Mazin H. Alwash and my sister Mrs. Hadeel H. Alwash and my brother in law Mr. Zaid H. Rasheed and their entire families.

Sincere appreciation to my perfect friend Mr. Ali Sabri Badday for his support and encouragement along the difficult times of my work. He was like guardian angel around me to facilitate all the difficulties. Also a special thanks to my friend Miss. Nur Azimah Jamulluddin for her help and advice throughout my PhD. Study. Finally, I appreciate every one helped at diverse levels to see the success of this work.

Atheel Hassan Alwash

USM, Penang, April 2013

## TABLE OF CONTENTS

<b>ACKNOWLEDGEMENTS</b>	ii
<b>TABLE OF CONTENTS</b>	iv
<b>LIST OF TABLES</b>	x
<b>LIST OF FIGURES</b>	xii
<b>LIST OF SYMPOLS</b>	xviii
<b>LIST OF ABBREVIATIONS</b>	xx
<b>ABSTRAK</b>	xxii
<b>ABSTRACT</b>	xxiv
<b>CHAPTER ONE- INTRODUCTION</b>	
1.1 Textile dyes	1
1.2 Wastewater treatment technology	2
1.3 Ultrasonic process	3
1.4 Sonocatalytic process	4
1.5 Problem Statement	6
1.6 Research objectives	8
1.7 Scope of study	9
1.8 Organization of thesis	9
<b>CHAPTER TWO- LITERATURE REVIEW</b>	
2.1 Advanced oxidation process (AOPs)	11
2.2 Principles of ultrasonic process	12
2.3 Effect of chemicals additives on the ultrasonic reaction	15
2.4 Combination of ultrasound with other processes	18
2.5 Sonocatalytic reaction	20

2.6	Zeolite as a molecular sieve support	22
2.6.1	TiO <sub>2</sub> loaded on different supports	24
2.7	The parameters affecting on the sonocatalytic reaction	29
2.7.1	Effect of pH	29
2.7.2	Effect of catalyst loading	34
2.7.3	The effect of doping metals	37
2.8	Stability of the catalyst	40
2.9	Mechanism of reaction	42
2.10	The kinetics of reaction	46

### **CHAPTER THREE-MATERIALS AND METHODS**

3.1	Introduction	50
3.2	Equipment, materials and chemicals	50
3.3	Preparation of catalyst	54
3.3.1	Preparation of Na-Y zeolite	54
3.3.2	Encapsulation of TiO <sub>2</sub> into Na-Y zeolite	54
3.3.3	Introduction of La (III) ions into the encapsulated TiO <sub>2</sub>	55
3.3.4	Preparation the Fe (III)/Ti <sub>4</sub> -NaY by impregnation method	55
3.3.5	Incorporation of Fe <sup>3+</sup> and TiO <sub>2</sub> into NaY	56
3.3.6	Incorporation of Fe <sup>3+</sup> and TiO <sub>2</sub> into NaY using tetrabutyl orthotitanate as titanium precursor	56
3.4	Characterization of the catalysts	57
3.4.1	Nitrogen adsorption-desorption isotherms	57
3.4.2	Inductive coupled plasma (ICP)	57
3.4.3	X-ray diffraction	58

3.4.4	Scanning electron microscopy (SEM) with energy dispersive X-ray (EDAX)	58
3.4.5	Fourier transforms infrared (FTIR) spectrometry	59
3.4.6	UV-Vis diffuse reflectance spectroscopy	59
3.4.7	Transmission electron microscope (TEM)	61
3.4.8	Atomic force microscopy (AFM)	61
3.4.9	Thermal gravimetric analysis (TGA)	62
3.5	Sonocatalytic Reaction	62
3.6	Chemical oxygen demand COD	64
3.7	The hydrophilic test	65
3.8	Remaining amount of H <sub>2</sub> O <sub>2</sub> at the end of reaction	65
3.9	Atomic absorption spectroscopy (AAS) technique	66
3.10	Reusability study of the catalyst	66
3.11	Kinetic study	67
	<b>CHAPTER FOUR- RESULTS AND DISSCUSION</b>	68
4.1	Development of functionalized Na-Y using Ti, La and Fe ions as doping metals	69
4.2	TiO <sub>2</sub> encapsulation into NaY followed by loading of La or Fe on the external surface of NaY: Characterization, activity and reusability study	69
4.2.1	Inductive coupled plasma (ICP) analysis	70
4.2.2	Surface characteristic of the prepared sonocatalysts	71
4.2.3	X-ray diffraction (XRD) measurement of the developed sonocatalyst	75
4.2.4	Scanning electron microscopy SEM with energy dispersive X-ray (EDAX)	80

4.2.5	UV-vis diffuse reflectance spectra analysis	85
4.2.6	Fourier transformed infrared spectroscopy (FTIR) analysis	90
4.2.7	Atomic force microscopy (AFM)	95
4.2.8	Transmission electron microscope (TEM)	98
4.3	Sonocatalytic degradation of Amaranth dye using titanium encapsulated into zeolite	100
4.3.1	Sonocatalytic activity of titanium encapsulated into zeolite	100
4.3.2	Effect of La loading on titanium oxide encapsulated into NaY	102
4.3.3	Effect of Fe loading on titanium oxide encapsulated into NaY	104
4.3.4	Control experiment	107
4.3.5	Effect of pH on decolorization of amaranth	110
4.3.6	Effect of catalyst dosage	113
4.3.7	Effect of hydrogen peroxide on decolorization of amaranth	116
4.3.8	Effect of dye concentration on decolorization efficiency of amaranth	118
4.3.9	Reusability and stability of the 0.8 % Fe/Ti <sub>4</sub> -NaY catalyst	121
4.4	Incorporation of TiO <sub>2</sub> and Fe <sup>3+</sup> into NaY in one single step using impregnation method. Characterization activity and reusability study	128
4.5	Catalyst characterization	128
4.5.1	Surface characteristic of the prepared sonocatalyst	129
4.5.2	X-ray diffraction (XRD) measurement of the developed catalyst	132
4.5.3	Thermal gravimetric analysis (TGA)	136



4.5.4	Scanning electron microscopy (SEM) with energy dispersive X-ray (EDAX)	138
4.5.5	UV-vis diffuse reflectance spectra of the sonocatalysts	140
4.5.6	Fourier transform infrared spectroscopy (FTIR) analysis	142
4.5.7	Atomic force microscopy (AFM)	144
4.6	Effect of co-incorporation of Fe <sup>3+</sup> and TiO <sub>2</sub> into zeolite on sonocatalytic activity	148
4.6.1	Control experiment	151
4.6.2	Effect of pH on decolorization of amaranth	153
4.6.3	Effect of catalyst loading	156
4.6.4	Effect of H <sub>2</sub> O <sub>2</sub> concentration	158
4.6.5	Effect of initial dye concentration	160
4.6.6	Reusability and stability of the 0.4 % Fe/15% TiO <sub>2</sub> -NaY catalyst	162
4.7	Incorporation of Fe <sup>3+</sup> and TiO <sub>2</sub> into NaY using impregnation method: Effect of titanium precursor on the characteristics, activity and reusability study	167
4.8	Catalytic characterization	167
4.8.1	Surface analysis of the sonocatalysts	168
4.8.2	X-ray diffraction (XRD) measurement of the developed catalyst	169
4.8.3	UV-vis diffuse reflectance spectra of the sonocatalysts	171
4.8.4	Atomic force microscopy (AFM)	172
4.9	Effect of incorporation of TiO <sub>2</sub> and a fixed amount of Fe into the zeolite on sonocatalytic activity	174
4.9.1	The reusability and stability of the 0.6 % Fe/10% TBT-NaY catalyst	180
4.10	The hydrophilic properties of the catalyst	184

4.11	Decolorization efficiency of different dyes using different types of catalyst	187
4.12	Role of radicals in the ultrasonic reaction	194
4.13	Residual amount of H <sub>2</sub> O <sub>2</sub> at the end of reaction	198
4.14	Comparative study between the modified catalyst 0.6 %Fe/10%TBT-NaY and other heterogeneous catalysts	201
4.15	Kinetic Model	204
4.15.1	Determination the kinetic parameters	204
<b>CHAPTER FIVE- CONCLUSIONS AND RECOMMENDATIONS</b>		
5.1	Conclusions	214
5.2	Recommendations for Further Research.	218
<b>REFERENCES</b>		219
<b>APPENDIXES</b>		
	Appendix A	242
	Appendix B	245
	Appendix C	247
	<b>List of Publications</b>	251

<b>LIST OF TABLES</b>		<b>Page</b>
Table 2.1	The ultrasonic process combined with other advanced oxidation processes.	19
Table 2.2	Effect of preparation method on the position of TiO <sub>2</sub> loaded on different supports	28
Table 2.3	Effect of pH on sonocatalytic degradation of various types of dyes.	33
Table 3.1	Chemicals and their properties used in this study with their respective roles.	52
Table 3.2	The structure and chemical properties of the models organic pollutants.	53
Table 4.1	ICP results for actual amounts of Ti species encapsulated into NaY using ion exchange procedure.	71
Table 4.2	BET surface area and pore volume data for the parent zeolite and different modified catalysts.	74
Table 4.3	Crystal analysis results of the developed sonocatalysts.	79
Table 4.4	The band gap energy values for different samples after the loading of La or Fe ions into the titanium encapsulated zeolite (Ti <sub>4</sub> -NaY).	89
Table 4.5	Results of the leaching test for the reuse catalyst 0.8%Fe/Ti <sub>4</sub> -NaY measured using AAS.	126
Table 4.6	Chemical compositions of the fresh catalyst and used 0.8%Fe/Ti <sub>4</sub> -NaY catalyst with and without calcination after three cycles of use for the decolorization of amaranth.	127
Table 4.7	BET surface area and pore volume data for the parent zeolite and different modified catalysts.	131
Table 4.8	Crystal analysis results of the developed sonocatalysts.	135
Table 4.9	Weight loss of the sample at different temperature ranges as determined using TGA under air flow.	138
Table 4.10	The leaching test for the reuse catalyst 0.4%Fe/15%TiO <sub>2</sub> -NaY as measured using AAS.	164

Table 4.11	Chemical compositions of the fresh catalyst 0.4%Fe/15%TiO <sub>2</sub> -NaY and used catalyst with and without calcination after three cycles of use for the decolorization of amaranth.	165
Table 4.12	The leaching test for the reuse catalyst 0.6%Fe/10%TBT-NaY as measured by using AAS.	182
Table 4.13	The chemical composition of the fresh catalyst and used 0.6%Fe/10%TBT-NaY catalyst with and without calcination after three cycles of use for the decolorization of amaranth.	183
Table 4.14	Comparative study between the performance of the synthesized catalyst and different types of catalysts reported in photocatalytic reaction.	203
Table 4.15	Reaction rate equations and their respective integral form.	205
Table 4.16	Determination of the reaction order with corresponding constant which best fit the data for different initial concentrations of amaranth dye under ultrasonic irradiation in the presence of 0.8% Fe/Ti <sub>4</sub> -NaY.	207
Table 4.17	Determination of the reaction order with corresponding constant which best fit the data for different initial concentrations of amaranth dye under ultrasonic irradiation in the presence of 0.6% Fe/10%TBT - NaY.	208
Table B.1	The absorbance values of the samples measured by UV-vis.	245
Table B.2	The concentration of the samples calculated from the calibration curve.	246
Table B.3	The decolorization efficiency of amaranth using 0.8%Fe/Ti <sub>4</sub> -NaY catalyst.	246

<b>LIST OF FIGURES</b>		<b>Page</b>
Figure 1.1	Creation of stable cavitation bubbles and creation and collapse of transient and stable cavitation bubbles. (a) Displacement (x) graph; (b) transient cavitation; (c) stable cavitation; (d) pressure (P) graph.	4
Figure 2.1	The reaction mechanism at three different zones i) inside cavitation bubble ii) bubble liquid interface and iii) liquid bulk.	12
Figure 2.2	Growth and implosion of cavitation bubble in aqueous solution with ultrasonic process.	13
Figure 2.3	Faujasite supercavities (R-cages) constructed of sodalite cages and hexagonal prism subunits with the charge compensating cations occupying different crystallographic positions are designated by Roman numerals.	24
Figure 2.4	The point of zero charge for a given mineral surface.	29
Figure 3.1	Flow diagram of the process.	51
Figure 3.2	Schematic diagram of the ultrasonic reaction system.	63
Figure 4.1	Physisorption isotherm for (a) NaY, (b) Ti <sub>4</sub> -NaY, (c) 0.64%LaTi <sub>4</sub> -NaY and (d) 0.8% Fe/Ti <sub>4</sub> -NaY.	73
Figure 4.2	The XRD results of different types of catalyst.	76
Figure 4.3	XRD patterns of parent NaY, titanium encapsulated zeolite (Ti <sub>4</sub> -NaY) and different concentrations of Fe loaded on Ti <sub>4</sub> -NaY.	78
Figure 4.4	SEM micrograph of different sonocatalyst (a,b) NaY, (c,d) Ti <sub>4</sub> -NaY, (e,f) La/Ti <sub>4</sub> -NaY, (g,h) 0.8%Fe/Ti <sub>4</sub> -NaY.	81
Figure 4.5	EDX result of (a) Ti <sub>4</sub> -NaY, (b) La/Ti <sub>4</sub> -Na and (c) 0.8 Fe/Ti <sub>4</sub> -NaY.	84
Figure 4.6	Effect of TiO <sub>2</sub> encapsulation into zeolite on the UV-vis reflectance spectra.	86
Figure 4.7	Effect of La ions on UV-vis reflectance spectra.	87
Figure 4.8	Effect of Fe ions incorporation on the UV-vis reflectance spectra.	88

Figure 4.9	The FTIR of (a) NaY, (b) Ti <sub>2</sub> -NaY and (c) Ti <sub>4</sub> -NaY.	91
Figure 4.10	FTIR spectra of (a) Ti <sub>4</sub> -NaY, (b) 0.64% La/Ti <sub>4</sub> -NaY and (c) 1.32% La/Ti <sub>4</sub> -NaY.	93
Figure 4.11	FTIR spectra of (a) Ti <sub>4</sub> -NaY, (b) 0.2% Fe/Ti <sub>4</sub> -NaY, (c) 0.4% Fe/Ti <sub>4</sub> -NaY, (d) 0.6% Fe/Ti <sub>4</sub> -NaY and (e) 0.8% Fe/Ti <sub>4</sub> -NaY.	94
Figure 4.12	The AFM (a) 3-D images followed by (b) 2-D images for the catalysts.	96
Figure 4.13	TEM images of (a,b) NaY at 8 and 45 k of magnification respectively, encapsulated titanium (c) Ti <sub>4</sub> -NaY, (d) 0.64 %La/Ti <sub>4</sub> -NaY and (e) 0.8 % Fe/Ti <sub>4</sub> -NaY.	99
Figure 4.14	Effect of titanium oxide concentration on the decolorization efficiency of amaranth (initial dye concentration of 10 mg/L, pH 5.5 and catalyst dosage 1.5 g/L).	101
Figure 4.15	The effect of different wt. % of La ions loaded on Ti <sub>4</sub> -NaY on decolorization efficiency of amaranth (initial dye concentration of 10 mg/L, pH 5.5 and catalyst dosage 1.5 g/L).	103
Figure 4.16	Effect of different concentrations of Fe <sup>3+</sup> ions loaded into Ti <sub>4</sub> -NaY on the decolorization efficiency of amaranth (initial dye concentration of 10 mg/L, pH 5.5 and catalyst dosage 1.5 g/L).	105
Figure 4.17	Preliminary study for decolorization of amaranth under various conditions. (Initial dye concentration 10 mg/L, catalyst loading 1.5 g/L and original pH).	108
Figure 4.18	Effect of pH on the decolorization efficiency of amaranth (Initial dye concentration 10 mg/L, catalyst loading 1.5 g/L, 0.2 M H <sub>2</sub> O <sub>2</sub> ).	111
Figure 4.19	Effect of catalyst dosage on the decolorization efficiency of amaranth. (Initial dye concentration 10 mg/L, pH 2.5, 0.2 M H <sub>2</sub> O <sub>2</sub> ).	115
Figure 4.20	Effect of H <sub>2</sub> O <sub>2</sub> concentration on the decolorization efficiency of amaranth. (Initial dye concentration 10 mg/L, pH 2.5, catalyst dosage 2 g/L).	117
Figure 4.21	Effect of initial dye concentration on decolorization efficiency (pH 2.5, catalyst dosage 2 g/L and 0.2 M of H <sub>2</sub> O <sub>2</sub> ).	119

Figure 4.22	Absorbance spectra for the decolorization of 10 mg/L amaranth dye by 0.8 % Fe/Ti <sub>4</sub> -NaY catalyst.	121
Figure 4.23	The decolorization efficiency and the COD removal for the fresh and used catalysts (10 mg/L initial dye concentration, pH 2.5, 0.2 M H <sub>2</sub> O <sub>2</sub> and 2.0 g/L of catalyst loading).	122
Figure 4.24	The XRD diffraction of fresh and used 0.8%Fe/Ti <sub>4</sub> -NaY catalyst.	123
Figure 4.25	Surface morphology of fresh catalyst (a) 0.8% Fe/Ti <sub>4</sub> -NaY and that of the used catalyst with calcination 0.8% Fe/Ti <sub>4</sub> -NaY (b) and (c) without calcination.	124
Figure 4.26	The adsorption – desorption isotherm of (a) NaY and (b) 0.4%Fe/15%TiO <sub>2</sub> -NaY	130
Figure 4.27	X-ray diffraction patterns of different catalysts used in this study.	132
Figure 4.28	TGA results of the catalyst and titanium precursor.	137
Figure 4.29	Surface morphology of (a) NaY and (b) 0.4% Fe/15%TiO <sub>2</sub> -NaY.	139
Figure 4.30	EDX analysis of 0.4%Fe/15%TiO <sub>2</sub> -NaY.	140
Figure 4.31	Diffuse-reflectance spectra of different types of catalysts.	141
Figure 4.32	FTIR spectra of different types of catalyst.	143
Figure 4.33	AFM images for different types of catalyst (a) three dimension and (b) two dimension.	146
Figure 4.34	Effect of interaction between (a) different loadings of Fe and fixed amount of TiO <sub>2</sub> with zeolite and (b) different loadings of TiO <sub>2</sub> and fixed amount of Fe with zeolite.	150
Figure 4.35	Preliminary study for the decolorization of amaranth dye under various conditions (initial dye concentration 10 mg/L, catalyst loading 1.5 g/L and original pH 5.5).	152
Figure 4.36	Effect of pH on the decolorization efficiency of amaranth dye, (initial dye concentration 10 mg/L, catalyst loading 1.5 g/L, 0.65 mM H <sub>2</sub> O <sub>2</sub> ).	154
Figure 4.37	Effect of catalyst loading on the decolorization efficiency of amaranth dye, (initial dye concentration 10 mg/L, pH 5.5, 0.65 mM H <sub>2</sub> O <sub>2</sub> ).	157

Figure 4.38	Effect of H <sub>2</sub> O <sub>2</sub> addition on the decolorization efficiency of amaranth dye,(initial dye concentration 10 mg/L, pH 5.5, catalyst dosage 2 g/L).	159
Figure 4.39	Effect of initial dye concentration on the decolorization efficiency of amaranth dye, (pH 5.5, and catalyst dosage of 2 g/L and 0.6 mM of H <sub>2</sub> O <sub>2</sub> ).	160
Figure 4.40	Decolorization efficiency of amaranth for the fresh and used catalyst after three reuse cycles (initial dye concentration 30 mg/L, pH 5.5, 0.65 mM H <sub>2</sub> O <sub>2</sub> and catalyst loading 2.0 g/L).	163
Figure 4.41	The XRD diffraction results for the fresh and used catalysts.	166
Figure 4.42	The adsorption-desorption isotherm for 0.6%Fe/10%TBT-NaY.	169
Figure 4.43	The XRD reflection of different types of catalyst synthesized using TBT precursor.	170
Figure 4.44	The diffuse reflectance spectra of different types of catalyst synthesized using TBT precursor.	172
Figure 4.45	Two and three dimension of AFM images for different types of catalyst used.	173
Figure 4.46	Effect of different loadings of TiO <sub>2</sub> and fixed amount of Fe in zeolite on decolorization of amaranth dye (initial dye concentration 10 mg/L, pH 2.5 and a catalyst loading 1.5 g/L) .	175
Figure 4.47	Color change of the catalyst (a) after 30 min of mechanical stirring and (b) at the end of ultrasonic reaction.	177
Figure 4.48	Effect of different loadings of Fe and a fixed amount of TiO <sub>2</sub> in zeolite on the decolorization of amaranth dye (initial dye concentration 10 mg/L, pH 2.5 and a catalyst loading 1.5 g/L).	178
Figure 4.49	Absorbance spectra for the decolorization of 10 mg/L amaranth dye by 0.6 % Fe/10%TBT-NaY catalyst.	179
Figure 4.50	The decolorization efficiency of the fresh and reused catalysts (initial dye concentration 10 mg/L, 2.5 pH and 1.5 g/L catalyst loading).	180
Figure 4.51	The XRD for the fresh and used catalysts.	181
Figure 4.52	Effect of hydrophilic/hydrophobic properties of the catalysts on the absorption of salicylic acid in hexane.	185



Figure 4.53	The decolorization efficiency of congo red using 0.8%/Fe/Ti <sub>4</sub> -NaY under ultrasonic reaction (initial dye concentration of 10 mg/L, a catalyst loading of 2.0 g/L and of 0.2 M of H <sub>2</sub> O <sub>2</sub> ).	189
Figure 4.54	The decolorization efficiency of congo red using 0.6%/Fe/TBT-NaY under ultrasonic reaction (initial dye concentration of 10 mg/L, 1.5 g/L of catalyst loading).	191
Figure 4.55	The decolorization efficiency of RB4 using 0.8%/Fe/Ti <sub>4</sub> -NaY catalyst under ultrasonic reaction (initial dye concentration of 10 mg/L, a catalyst loading of 2.0 g/L and of 0.2 M of H <sub>2</sub> O <sub>2</sub> ).	193
Figure 4.56	The decolorization efficiency of RB4 using 0.6%/Fe/TBT-NaY catalyst under ultrasonic reaction (initial dye concentration of 10 mg/L, 1.5 g/L of catalyst loading).	193
Figure 4.57	Effect of radical's scavenger on decolorization efficiency of amaranth using 0.8%/Fe/Ti <sub>4</sub> -NaY under ultrasonic reaction.	195
Figure 4.58	Effect of radical's scavenger on the decolorization efficiency of amaranth using 0.6%Fe/10%TBT-NaY under ultrasonic reaction.	197
Figure 4.59	Residual amount of H <sub>2</sub> O <sub>2</sub> after 120 min of ultrasonic reaction for different types of dye.	199
Figure 4.60	Kinetic model of Okitsu <i>et al.</i> (2005).	211
Figure 4.61	The kinetics based Okitsu model for (a) 0.8%Fe/Ti <sub>4</sub> -NaY and (b) 0.6%Fe/10%TBT-NaY.	213
Figure A-1	Calibration curve for UV-vis spectrophotometric measurement of amaranth dye at low concentration.	242
Figure A-2	Calibration curve for UV-vis spectrophotometric measurement of amaranth dye at high concentration.	242
Figure A-3	Calibration curve for UV-vis spectrophotometric measurement of RB4 dye.	243
Figure A-4	Calibration curve for UV-vis spectrophotometric measurement of congo red dye at normal and basic pH.	243
Figure A-5	Calibration curve for UV-vis spectrophotometric measurement of congo red dye at acidic pH.	244

Figure A-6	Calibration curve for UV-vis spectrophotometric measurement of salicylic acid.	244
Figure C-1	Zero order reaction rate of 0.8% Fe loaded on encapsulated titanium for amaranth dye from (10-100) mg/L.	247
Figure C-2	First order reaction rate of 0.8% Fe loaded on encapsulated titanium for amaranth dye from (10-100) mg/L.	247
Figure C-3	Second order reaction rate of 0.8% Fe loaded on encapsulated titanium for amaranth dye from (30-100) mg/L.	248
Figure C-4	Third order reaction rate of 0.8% Fe loaded on encapsulated titanium for amaranth dye from (30-70) mg/L.	248
Figure C-5	Zero order reaction rate of 0.6% Fe/10%TBT-NaY for amaranth dye from (10-100) mg/L.	249
Figure C-6	First order reaction rate of 0.6% Fe/10%TBT-NaY for amaranth dye from (10-100) mg/L.	249
Figure C-7	Second order reaction rate of 0.6% Fe/10%TBT-NaY for amaranth dye from (30-100) mg/L.	250
Figure C-8	Third order reaction rate of 0.6% Fe/10%TBT-NaY for amaranth dye from (30-100) mg/L.	250

## LIST OF SYMBOLS

**Unit**

$A$	Absorbance	-
$C, C_t$	Concentration at any time	mg/L
$C_o$	Initial concentration	mg/L
$e^-$	Electron	-
$E_g$	Band-gap energy	eV
$h^+$	Hole	-
$h\nu$	Photon energy	eV
$H$	Hysteresis type	-
$k_1$	Adsorption rate constant	$\text{min}^{-1}$
$k_{-1}$	Desorption rate constant	$\text{M}\cdot\text{min}^{-1}$
$k$	Pseudo-rate constant	Depend on reaction order
$K$	Equilibrium constant	$\text{L}\cdot\text{mg}^{-1}$
$k_{\text{app}}$	Apparent rate constant	Depend on reaction order
$M$	Molarity	mg/L
$\cdot\text{OH}$	Hydroxyl radical	-
$\text{OH}^-$	Hydroxyl ion	-
$\text{H}^+$	Hydrogen ion	-
$P/P_o$	Relative pressure	-
$r, r_{\text{dye}}$	Rate of reaction	-
$r_o$	Initial rate of reaction	-

		<b>Unit</b>
R	Reflectance for any intermediate energy photon	-
$R^2$	Coefficient of determination	-
$R_{max}, R_{min}$	Maximum and minimum reflectance	-
t	Thin film thickness in reflectance spectra	-
$\alpha$	Absorption coefficient	-
$2\theta$	Bragg's angle in degree	-
$\theta$	Occupied ratio of pollutant	-
$\lambda$	Wavelength	nm

## LIST OF ABBREVIATIONS

AFM	Atomic force microscopy
Al <sub>2</sub> O <sub>3</sub>	Aluminum oxide
AOPs	Advanced oxidation processes
BET	Brunauer-Emmet-Teller
CB	Conduction band
CCl <sub>4</sub>	Carbon tetrachloride
Cds	Cadmium sulphide
CeO <sub>2</sub>	Cerium dioxide
CO <sub>2</sub>	Carbon dioxide
COD	Carbon oxygen demand
C <sub>12</sub> H <sub>28</sub> O <sub>4</sub> Ti	Titanium(IV) isopropoxide
C <sub>16</sub> H <sub>36</sub> O <sub>4</sub> Ti	Tetrabutyl orthotitanate (TBT)
EDAX	Energy dispersive X-ray
FT-IR	Fourier transforms infrared spectrometry
Fe <sub>2</sub> O <sub>3</sub>	Ferric oxide or Hematite
HCl	Hydrochloric acid
H <sub>2</sub> O <sub>2</sub>	Hydrogen peroxide
H <sub>3</sub> PW <sub>12</sub> O <sub>40</sub>	Phosphotungstic acid
HOCl	Hypochlorous acid
HNO <sub>3</sub>	Nitric acid
H <sub>2</sub> SO <sub>4</sub>	Sulfuric acid
HY	H-Y zeolite
ICP	Inductive coupled plasma

KBr	Potassium bromide
kHz	Kilohertz (ultrasonic frequency)
NaY	Na- Y zeolite
$(\text{NH}_4)\text{TiO}(\text{C}_2\text{O}_4)_2$	Ammonium titanyl oxalate
pm	Picometer (SI unit of length)
PTO	Potassium titanium oxalate
RB4	Reactive blue 4
TGA	Thermal gravimetric analysis
$\text{TiCl}_4$	Titanium tetrachloride
TEM	Transmission electron microscope
SEM	Scanning electron microscopy
$\text{SiO}_4$	Silicon tetraoxide
US	Ultrasonic
UV-vis	UV-Vis diffuse reflectance spectroscopy
UV	Ultra violet
VB	Valance band
W	Watt (Power of ultrasonic)
Wt. %	Weight percent
XRD	X-ray diffraction
ZnO	Zinc oxide
$\text{ZrO}_2$	Zirconium dioxide

**PENYEDIAAN DAN PENCIRIAN MANGKIN BERASASKAN ZEOLIT Y-  
UNTUK PENGURAIAN SONO MANGKIN PENCELUP  
ORGANIK DI DALAM AIR**

**ABSTRAK**

Proses mangkin bersono telah digunakan untuk meningkatkan proses penyahwarnaan dan pemineralan dan air sisa yang mengandungi pewarna (amaranth, reaktif biru 4 dan kongo merah). Zeolit Y telah digunakan sebagai bahan sokongan dan telah diubahsuai dengan menggunakan tiga logam aktif yang berbeza iaitu Ti, La dan Fe. Kedudukan titanium oksida (sama ada terkandung atau dimuatkan pada bahan sokongan) telah dikawal menggunakan kaedah penyediaan terpilih, iaitu pertukaran ion dan kaedah impregnasi. Sementara itu, logam La dan Fe telah disebarkan pada permukaan luar zeolit. Pengubahsuaian TiO<sub>2</sub> menggunakan logam Fe telah meningkatkan kecekapan penyahwarnaan amaranth dengan lebih baik berbanding dengan pengubahsuaian dengan logam La. Kecekapan penyahwarnaan yang maksimum adalah kira-kira 97% dengan penyingkiran maksimum COD adalah 57% selepas 120 minit tindak balas. Tindak balas pemangkin tersebut dibantu oleh sumber penyinaran ultrasonik pada tahap kuasa 50 W dengan frekuensi 40 kHz. Apabila kedudukan TiO<sub>2</sub> ditetapkan pada permukaan luar zeolit bersama-sama dengan logam Fe, mangkin menunjukkan kecekapan penyahwarnaan pewarna yang lebih tinggi iaitu hampir 100% selepas 120 minit. Semua kecekapan pemangkin yang telah diubahsuai telah dikaji dengan membandingkan aktiviti mereka dengan zeolit kosong dan mono-doping logam tunggal aktif dalam keadaan kajian yang sama. Parameter operasi yang berbeza telah disiasat iaitu kepekatan awal pencelup, pH awal, bebanan mangkin dan penambahan agen pengoksidaan seperti H<sub>2</sub>O<sub>2</sub>. Antara pelbagai keadaan tindak balas, pH menunjukkan pengaruh yang tinggi terhadap

proses ini. Mangkin bersono juga telah menjalani proses pencirian menerusi kaedah pembelauan sinar-X (XRD) dan Fourier bertukar infra merah (FTIR) untuk struktur dan analisis kumpulan berfungsi masing-masing, imbasan mikroskop elektron imbasan (SEM) untuk mikrostruktur dan morfologi, permukaan penjerapan fizik nitrogen bagi luas permukaan dan taburan saiz liang serta pantulan disebarakan UV-vis untuk penilaian perbezaan jalur. Penambahan logam Fe terhadap titanium Ti-NaY atau mangkin Fe/TiO<sub>2</sub> terhadap NaY menyebabkan pengurangan ketara dalam jurang jalur tenaga daripada 3.5 eV kepada 2.8 eV dan 2.75 eV bagi mangkin (0.8%Fe/Ti-NaY) dan mangkin (0.6%Fe/10%TBT-NaY) masing-masing. Sifat hidrofilik/hidrofobik dipengaruhi oleh kaedah penyediaan, sifat kation serta kepekatan logam dalam struktur zeolit. Mangkin bersono mempunyai luas permukaan yang tinggi dan N<sub>2</sub> penjerapan-desorption isoterma adalah dari Jenis I dengan gelung histerisis H4. Potensi pemangkin untuk diguna semula telah dipamerkan untuk beberapa kitaran berturut-turut. Kajian kinetik telah berjaya dijalankan dan tertib tindakbalas yang terbaik untuk keseluruhan proses adalah tertib pertama.



**PREPARATION AND CHARACTERIZATION OF ZEOLITE Y – BASED  
CATALYSTS FOR SONOCATALYTIC DEGRADATION OF  
ORGANIC DYES IN WATER**

**ABSTRACT**

Sonocatalytic process was adopted to enhance the decolorization and mineralization of wastewater containing dyes (amaranth, reactive blue 4 and congo red). Zeolite Y was used as the support material and modified using three different active metals i.e. Ti, La and Fe. The position of titanium oxide (either encapsulated or loaded on the support) was controlled using different preparation methods, e.g. ion exchange and impregnation methods. Meanwhile, La or Fe metals were deposited on the external surface of the zeolite. The modification of the encapsulated TiO<sub>2</sub> by Fe metal enhanced the decolorization efficiency of amaranth dye more efficiently than its modification with La metal. The maximum decolorization efficiency was about 97 % with maximum COD removal of 57 % after 120 min of reaction. The catalytic reaction was assisted by an ultrasonic irradiation source at 50 W for the output power and the frequency was 40 kHz. As the position of TiO<sub>2</sub> was replaced to be at the external surface of zeolite together with Fe metal, the catalyst also showed higher decolorization efficiency of amaranth about 100 % after 120 min of sonocatalytic reaction. All catalytic efficiencies of the modified catalysts were demonstrated by comparing their catalytic activity with that of bare zeolite and mono-doping of active metal with zeolite under the same experimental conditions. Different operational parameters were investigated for the best of higher catalytic activity such as initial pollutants concentration, initial pH, catalyst loading and the addition of oxidizing agents such as H<sub>2</sub>O<sub>2</sub>. Among various reaction conditions, the initial pH greatly influenced the sonocatalytic process in all cases. The developed

sonocatalysts were successfully characterized using X-ray diffraction (XRD) and Fourier transformed infrared (FTIR) for structural and functional groups analysis respectively, surface scanning electron microscopy (SEM) for microstructure and morphology, nitrogen-physisorption for surface area and pore size distributions and UV-vis diffused reflectance for band gap evaluation. The Fe ions loaded onto encapsulated titanium or Fe/TiO<sub>2</sub> loaded on NaY caused a significant reduction in band gap energy from 3.55 eV for bare TiO<sub>2</sub> to 2.8 and 2.75 for Fe loaded on encapsulated (0.8%Fe/Ti-NaY) and Fe/TiO<sub>2</sub> loaded NaY (0.6%Fe/10%TBT-NaY), respectively. The hydrophilic/hydrophobic properties were affected by the preparation method, the nature of cations as well as the concentration of metals in the zeolite structure. The sonocatalyst possessed high surface areas and N<sub>2</sub> adsorption-desorption isotherms was of type I with H4 hysteresis loops. The developed catalyst demonstrated high reusability potential for many consecutive cycles. The kinetic study was successfully conducted and it was revealed that reaction order best represented of the whole process was the first order.

# CHAPTER ONE

## INTRODUCTION

### 1.1 Textile dyes

Environmental pollution is commonly caused by the presence of hazardous and toxic materials such as dyes which is widely used in many industries such as textiles, printing, dyeing, and food coloring industries. Even at small amount, these dyes have the ability to produce a visible color which is considered a serious problem due to their negative effects on the water environment. In addition, some of these dyes are toxic and non-biodegradable and therefore they are also harmful to aquatic life (Wang *et al.*, 2008a).

Dye molecules generally consist of two key components i.e. the chromophores which are responsible for producing the color and the auxochromes which can not only complement the chromophore but also render the molecule soluble in water and give enhanced affinity (to attach) toward fibers (Gupta and Suhas, 2009). The colour imparted to water by dyes is visible to human eye and therefore, highly objectionable on aesthetic grounds.

Dyes cause damage to the environment because they prevent sunlight and oxygen penetration. Therefore, they can significantly affect photosynthetic activity in aquatic systems (Dizge *et al.*, 2008). In addition, dyes may affect human health due to oral ingestion and inhalation, skin and eye irritation, and skin sensitization leading to a serious problems in human health (Rai *et al.*, 2005). Therefore, a lot of effort has been dedicated to the development of different types of treatment processes in order to degrade the harmful compounds by converting them to small chemical products.

Dyes with their structural variety can be classified into several ways. These dyes can be classified according to their chemical structure or their application in the industrial process. Dyes can also be classified according to their solubility. However, the classification based on their usage is the most common such as acid dyes, basic dyes, disperse dyes, direct dyes, reactive dyes, solvent dyes, sulfur dyes and vat dyes (Hunger, 2007).

## **1.2 Wastewater treatment technology**

A wide range of treatment methods have been developed for the removal of dyes from water and wastewater to eliminate their harmful effect on environment. Generally, the wastewater treatment processes can be divided into three main categories namely biological, physical and chemicals treatments method (Nidheesh *et al.*, 2013). Different researchers have investigated various types of conventional wastewater treatment such as the coagulation and filtration (Unlu *et al.*, 2009), adsorption by activated carbon (Al-Degs *et al.*, 2008) and biological treatment (Kornaros and Lyberatos, 2006) for the removal of dyes from wastewater. However these traditional treatments process cause a secondary pollution, since the toxic substances transfer from the liquid phase to other phases such as the sludge, used membranes and saturated adsorbents that will cause another environmental problem. As a result, a great interest has been given to advanced oxidation processes (AOPs) due to the alternative destructive treatment in which the chemical species are reduced into smaller fragments and even to the point of mineralization. AOPs such as ozonation, photocatalysis, ultrasonic reaction, Fenton and a combination of photo-Fenton, UV/O<sub>3</sub> and UV/H<sub>2</sub>O<sub>2</sub> are novel technologies that have been widely developed to enhance their ability to generate the high reactive hydroxyl radicals ( $\cdot\text{OH}$ ) that have

a high efficiency to oxidize organic matters (Jamalluddin and Abdullah, 2011a). However, the high running cost is the main drawbacks of these processes. Thus, there is a need to use some additives either soluble ones such as Fenton /Fenton like reagents,  $H_2O_2$  and  $CCl_4$  or insoluble ones such as the heterogeneous catalysts in order to reduce the running cost and enhance the production of  $\cdot OH$  radicals (Güyer and Ince, 2011).

### **1.3 Ultrasonic process**

Among various types of AOPs, ultrasonic irradiation has been receiving a great attention in wastewater treatment processes. The ultrasonic sound is transmitted through any physical medium by waves. Once the ultrasound cross the medium (Figure 1.1) the average distance between the molecules will vary and oscillate about their mean position. When the change in pressure caused by ultrasonic wave is large enough, the distance between the molecules of the liquid exceeds the minimum molecular distance required to hold the liquid intact. Thus, the liquid breaks down and voids are created. Those voids are the so-called cavitation bubbles (Capelo-Martinez, 2009). During the ultrasonic process, the water molecules decomposed into extremely reactive hydrogen atoms ( $H^+$ ) and hydroxyl radicals ( $\cdot OH$ ) by the heat generated from the cavity implosion. This cavity implosion is responsible for the high localized temperature and pressure inside the bubble (Joseph *et al.*, 2009; Dehghani and Fadaei, 2013).

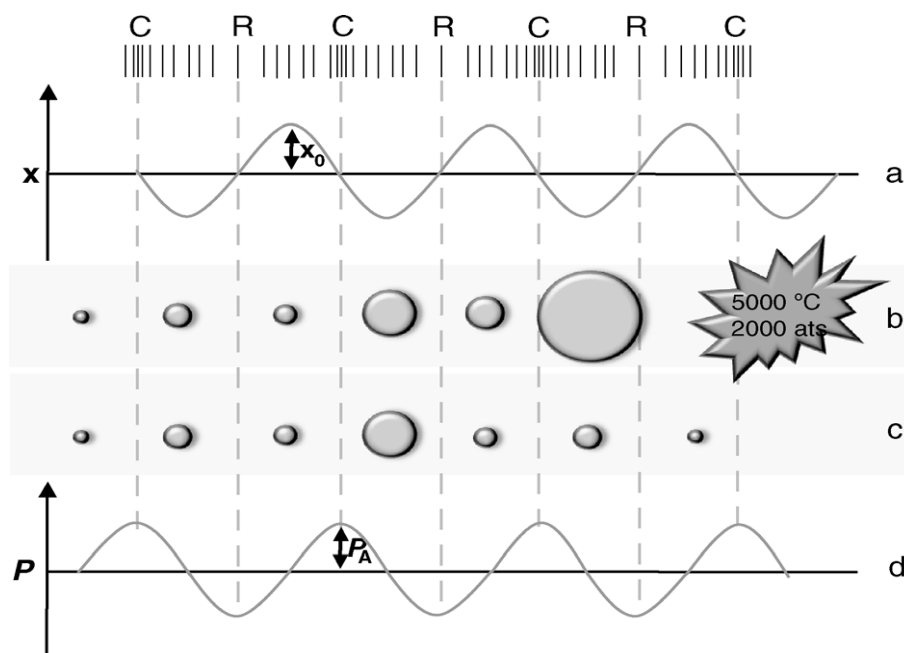


**Figure 1.1.** Creation of stable cavitation bubbles and creation and collapse of transient and stable cavitation bubbles. (a) Displacement ( $x$ ) graph; (b) transient cavitation; (c) stable cavitation; (d) pressure ( $P$ ) graph. (Capelo-Martinez, 2009).

#### 1.4 Sonocatalytic process

The synergetic effect between ultrasound irradiation and heterogeneous catalyst provides advantages in addition to the formation of radicals species through normal means. The ultrasonic process offer, clean reactive surfaces for the catalyst during the reaction by the removal of reactive intermediates or by-products from the catalyst surface. In addition, the division of the catalyst into small particles offers a higher surface area to allow higher mass transfer. This is considered as the main advantages of ultrasound-based system over other AOPs (Zhong *et al.*, 2011a).

Titanium oxide is one of the most important heterogeneous catalysts used in ultrasonic process owing to its non-toxic property, inexpensive and highly reactive nature under UV irradiation that has been widely adopted to oxidize dyes in wastewater as well as its high durability, corrosion resistance, and high oxidation

potential (Yamaguchi *et al.*, 2010). However, there are several limitations to use 'bare' TiO<sub>2</sub> due the recombination of e<sup>-</sup> - h<sup>+</sup> pair generated from the irradiated TiO<sub>2</sub> and its rapid aggregation in suspension resulting in smaller effective surface area and lower catalytic efficiency. Moreover, the recycling difficulties due to the small size of TiO<sub>2</sub> particles (Wang *et al.*, 2008a).

As a result, efforts have been recently focused on the modification of bare TiO<sub>2</sub>. One of the most efficient solutions is by doping of transition metals into the lattice of TiO<sub>2</sub> to inhibit the electron-hole recombination and many successful researches have been attempted in this field (Zou *et al.*, 2013; Shirsath *et al.*, 2013; Musa *et al.*, 2011).

Another efficient solution to modify the bare TiO<sub>2</sub> is by immobilizing it on different porous materials such as silica (Lee *et al.*, 2008) , carbon (Wantala *et al.*, 2013), glass (Kumar and Bansal, 2013) and zeolite (Petkowicz *et al.*, 2009) to solve the problems of limited surface area of TiO<sub>2</sub> and to eliminate the separation difficulties.

Among various investigated supports, TiO<sub>2</sub> supported zeolites have been widely investigated especially in photocatalytic reactions due to the ability of zeolite to accept the guest molecules either on the external surface or being encapsulated into their pores of zeolite. Nikazar *et al.* (2007); Liu *et al.* (1992) and Chen *et al.* (1999) and many other researchers have all concluded that the immobilization of TiO<sub>2</sub> on zeolites had a positive effect in increasing the photocatalytic activity of the catalysts for the degradation of organic compounds in water.

As such, the activity of the modified TiO<sub>2</sub> can be affected by several factors such as the dopant concentration, the location of energy levels of dopants in the lattice, the electronic configuration and distribution of dopants. In addition, the optical properties of pure TiO<sub>2</sub> and the preparation method of the doped metal with TiO<sub>2</sub> can affect greatly on the activity of the produced composite (Kernazhitsky *et al.*, 2008).

### **1.5 Problem Statement**

Dyes are non-biodegradable and highly soluble in water and their transfer into water medium is relatively easy compared to insoluble pollutants. Therefore, the degradation of dye wastewater has become a major environmental problem that needs to be solved to avoid their damaging effects on the environment. Much effort has been focused on producing different types of catalyst ranging from homogeneous to heterogeneous catalysts that have the ability not only to remove the color of the dyes from the wastewater but also to degrade these dyes and convert them to small harmless molecules.

Supported titanium oxides encapsulated or loaded onto zeolite have been widely investigated in photocatalytic reactions. However, the main drawback of the photocatalytic reaction is the need for suitable reactor design that can be suitable for large volume of water and optimum exposure of light to the solid surface. Furthermore, the problems of light penetration, scattering and diffraction can consequently cause the problem of long reaction time that can increase the cost of the running process.



Therefore, it is expected that the ultrasonic irradiation should be suitable to solve the problems of photocatalytic reaction due to several advantages such as the high penetrating depths of ultrasonic up to 20-30 cm comparing to the low penetrability during the photocatalytic process in water medium (limited to several millimeters), improvement in the diffusion of reactant from the bulk solution to the surface of catalyst, continuous cleaning of the catalyst surface which is ascribed to the desorption of the generated product during oscillation. In addition, ultrasonic process prevents the aggregation of the catalyst particles due to the fragmentation of the particles into smaller sizes thus increasing the active surface area available for the reaction. The use of heterogeneous catalyst in combination with ultrasonic irradiation can be considered a good solution to further minimize the cost of the process by reducing the reaction time. The selection of zeolite as a support is ascribed to the special properties of zeolite i.e. high internal and external surface area, its ability to accept more than one guest molecules, good thermal stability, high absorption ability to organic compounds and the existence of acid-base sites in the framework structure which describes their electron accepting-donating properties.

As a result, the synergistic between metals i.e. La or Fe /TiO<sub>2</sub> with zeolite should enhance the sonocatalytic activity for the degradation of dyes under ultrasonic reaction. The function of TiO<sub>2</sub> is to generate e<sup>-</sup> - h<sup>+</sup> pairs into the reaction that will facilitate the generation of free radicals. However, the existence of La or Fe ions in the supported TiO<sub>2</sub> will play two different roles. The Fe ion acts as electron acceptor to inhibit the recombination of e<sup>-</sup> - h<sup>+</sup> pairs. Besides, it is considered as an effective Fenton-like catalyst and its synergistic effect with TiO<sub>2</sub> as a common photocatalyst should enhance the sonocatalytic activity. The role of La is to help in reducing the

energy gap of the titanium oxide and inhibit the recombination of the  $e^- - h^+$  pairs that are produced from the irradiated catalyst. The synergetic effects between the catalyst and ultrasonic process are theoretically believed to enhance the efficiency of the degradation process. The presence of ultrasound will also be useful in providing the mechanical vibration effect to the solution and to activate the catalyst to produce the efficient hydroxyl radicals. It is also responsible for the removal of reactive intermediates or by-products from the catalyst surface, thereby, providing clean and reactive surfaces for subsequent reactions over the heterogeneous catalytic systems.

To the best of our knowledge, no report is available in literature on the immobilization of  $TiO_2$  on zeolite to be used in ultrasonic-assisted AOPs. Therefore, the current study focuses on differences in characterization and catalytic performance of various modified zeolites by the co-doping of metals and  $TiO_2$  into/onto zeolite for use in the sonocatalytic degradation of dyes using ultrasound- assisted process.

### **1.6 Research objectives:**

- 1- To modify the function of zeolite Y using  $TiO_2$  combined with two metals i.e. La and/or Fe for the degradation of dyes in water under ultrasonic reaction.
- 2- To fully characterize the modified catalysts and compare them with unsupported one in order to identify and elucidate changes in physical and chemical properties after the modification.
- 3- To study the reaction conditions of the sonocatalytic process that will affect the efficiency of the degradation process of the dyes.

- 4- To study the reusability of the synthesized catalysts after several consecutive reactions cycles.
- 5- To study the kinetics of reaction for the catalytic degradation of dye under the ultrasonic-assisted process.

### **1.7 Scope of study**

The study focuses on the use of zeolite Y as a support for the incorporation of TiO<sub>2</sub> combined metals such as La or Fe for the degradation of dyes i.e. amaranth, congo red and reactive blue 4 using sonocatalytic process. The study also involves extensive characterization of the developed catalysts to investigate and elucidate the chemical and physical changes that occur after the modification step and evaluation the effect of different reaction parameters on the sonocatalytic activity. Furthermore, the characterization of the catalyst and catalytic activity after many cycles of use is also conducted. The kinetics of reaction is also carried out to elucidate the reaction rate order and to investigate the postulated reaction occurrence.

### **1.8 Organization of the thesis**

This thesis consists of five chapters. The first chapter discussed the effect of the dyes on the environment and also covers some history on the treatment method used in the wastewater treatment processes until the creation of the advanced oxidation process (AOPs) which are widely used in industry currently. The problem statement, objectives and the scope of this study are also provided in this chapter.

Chapter two present a literature survey for the published reports in the field of the degradation of dyes in water. The chapter presents in details the principles of ultrasonic process, the synergistic effect with the addition of certain chemicals with

ultrasonic irradiation, the effect of combination between the heterogeneous catalyst with ultrasonic process and the effect of reaction parameters on the sonocatalytic activity. The chapter also reviews the potential for the reusability of the heterogeneous catalyst in addition to the kinetics and mechanism of reaction.

Chapter three (Materials and Methods) present the experimental information of the current study in details including all the chemical and materials used during the experimental works, the catalyst preparation methods, the characterization techniques used to investigate the physical and chemicals properties of the produced catalysts as well as to the analytical procedures used for the catalytic activity.

Chapter four (Results and Discussion) analyze in details all the results obtained from the present investigation. This chapter is divided into eight major sections; TiO<sub>2</sub> encapsulation into NaY followed by loading of La or Fe ions, incorporation of TiO<sub>2</sub> and Fe ions with NaY in one single step using impregnation method and the incorporation of TiO<sub>2</sub> and Fe ions into NaY using tetra butyl orthotitanate as TiO<sub>2</sub> precursor. All the previous studies were included the characterization, catalytic activity and reusability study. Furthermore, the chapter presents the investigation of the hydrophilic properties of the prepared catalyst, decolorization efficiency of different dyes using different types of catalyst, investigate the effect of radical scavengers on the sonocatalytic activities of the produced catalysts, investigate the residual amount of H<sub>2</sub>O<sub>2</sub> remained at the end of reaction and kinetics model. In Chapter five (Conclusions and recommendations), the discussion made in this study and recommendations for the future studies in this field were elucidated.

## CHAPTER TWO

### LITERATURE REVIEW

#### 2.1 Advanced oxidation process (AOPs)

Advanced oxidation process (AOPs) are considered alternative methods to conventional wastewater treatment technologies due to the high oxidizing efficiency of various types of organic compound by hydroxyl radicals generated during the process. Furthermore the AOPs is a green technology due to the low- or non- waste generating after the end of the process which is one of the main drawbacks of the traditional wastewater treatment processes (Aleksić *et al.*, 2010). The AOPs can be classified according to the type of the energy source applied during the reaction e.g. ozonation process (Tehrani-Bagha *et al.*, 2010), photochemical or photocatalytic process (Zhou *et al.*, 2013), Fenton process (Bouasla *et al.*, 2010 and Sun *et al.*, 2007b), electrichemical process (Kalathil *et al.*, 2013) and ultrasonic process (Kobayashi *et al.*, 2012). AOPs involve the two stages of oxidation i.e. the formation of strong oxidants (hydroxyl radicals) and the reaction of these oxidants with organic contaminants in water. The hydroxyl radicals are chemically unstable reactive species due to their unpaired electrons. Therefore, a continuous oxidation reaction between these unstable radicals and other reactant e.g. organic and inorganic compounds until thermodynamically stable oxidation products are formed (Deforman and Adams, 1973).

## 2.2 Principles of ultrasonic process

The main principles of the process start from the transition of ultrasonic sound waves in the range of 20-1000 kHz throughout an aqueous solution to create what is known as an acoustic cavitation. The high magnitude of energy generated during the sonolysis is process ascribed to the formation of the small size bubbles which then grow and subsequently collapse in split seconds (Joseph *et al.*, 2009) as seen in Figures. 2.1 and 2.2 leading to the generation of many local hot spots with extremely high temperature (up to 5000 K) and high pressure (up to 1000 atm.) that consequently induce the dissociation of water (Eqs. 1- 4) (Abdullah and Ling, 2010).

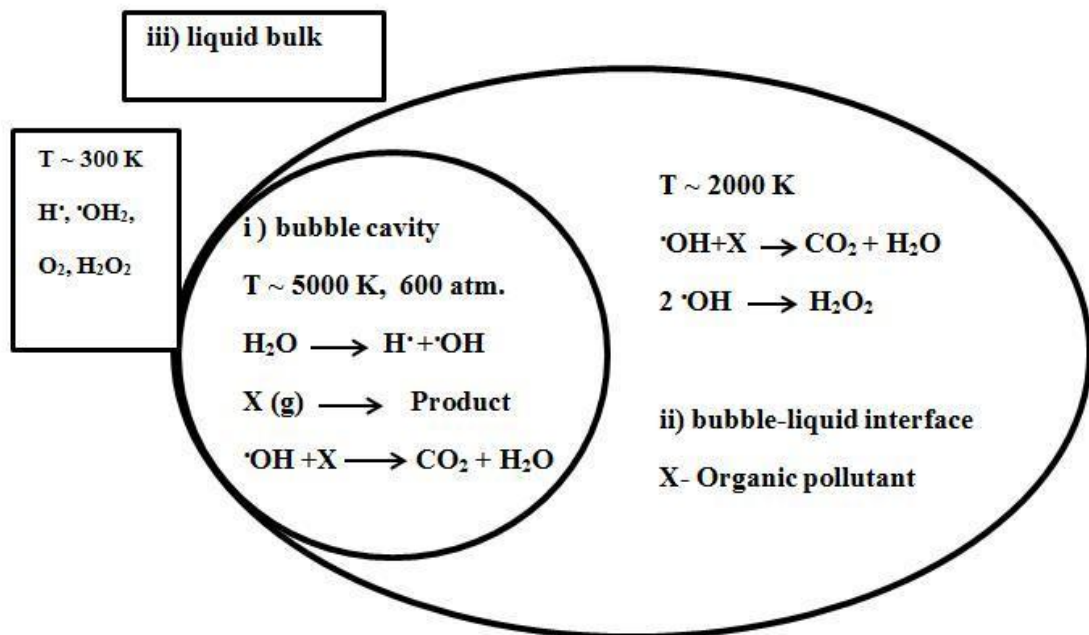


**Figure 2.1.** The reaction mechanism at three different zones i) inside cavitation bubble ii) bubble liquid interface and iii) liquid bulk (Joseph *et al.*, 2009).

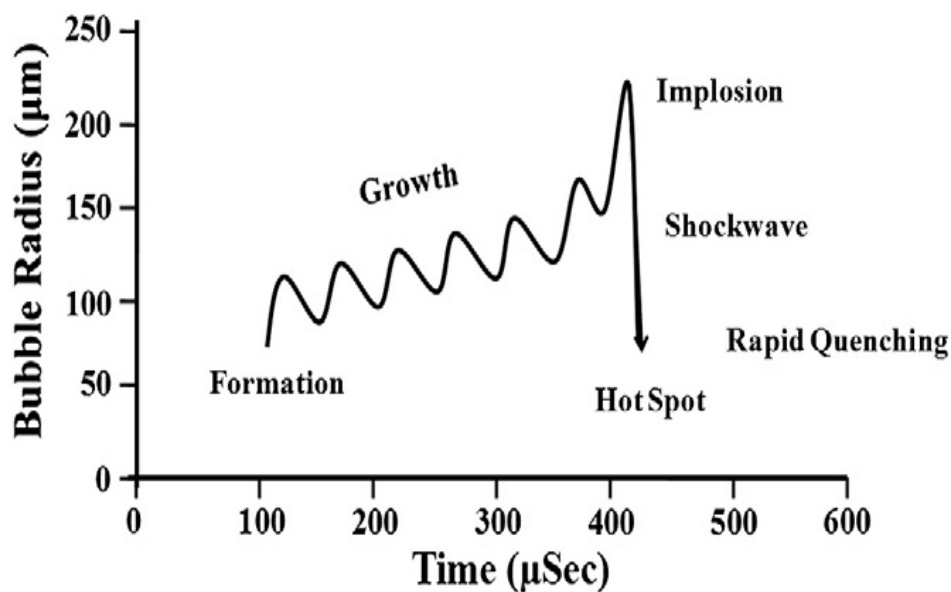


**Figure 2. 2.** Growth and implosion of cavitation bubble in aqueous solution with ultrasonic process (Suslick, 1989).



The use of ultrasound presents unique advantages such as enhancement of mass transfer and reaction rates, improvement of surface properties, lowering of chemical consumption and sludge generation rates and promoting the generation of  $\cdot\text{OH}$  radicals (Ince *et al.*, 2001). The formation of  $\cdot\text{OH}$  radicals can take place during the pyrolysis inside the cavity bubble or near the interface and surrounding the liquid. These radicals are responsible for the oxidation of organic compounds to ultimately convert them into  $\text{CO}_2$  and  $\text{H}_2\text{O}$  (Mahamuni and Adewuyi, 2010).

Several successful research works have been reported on the effect of ultrasound on the degradation of organic compounds such as organic dyes (Kobayashi *et al.*, 2012; Wang *et al.*, 2008d; Yao *et al.*, 2010; Patidar *et al.*, 2012; Sáez *et al.*, 2011). The effect of ultrasonic process on the decolorization and degradation of reactive and basic dyes have been reported by Tezcanli-Guyer and Ince (2003) using high ultrasonic frequency of 520 kHz. The results indicated that the  $\cdot\text{OH}$  radicals formed during the reaction had the tendency to attack the azo bonds (N=N) faster than the degradation of organic and olefinic compounds. This behavior could be ascribed to the formation of more intermediate products during the reaction that made the degradation step for organic compound slower than the color removal.

The ultrasound has advantage to divide the solid particles such as the insoluble dyes molecules that have high molecular weight in solution into finer ones (in nano meter size range) and eliminate their aggregation. This behavior is ascribed to the mechanical vibration properties provided by ultrasound. Lee *et al.* (2001) reported an investigation about the ability of ultrasonic waves in reducing the size of insoluble dye molecules suspended in water into finer particles. The results showed that the specific breakage rate for dye particles irradiated by ultrasound depends on their crystalline properties thus, the more crystallized dye the higher breakage rate.

The use of ultrasonic alone without any catalyst or additives may be not suitable for all kinds of pollutant due to various variables such as the power of ultrasound, the chemical structures and the size of the pollutant molecules. Therefore, there is a need to accelerate the process by adding additives such as salts or organic



solvents to increase the production of  $\cdot\text{OH}$  radicals which enhance the degradation process.

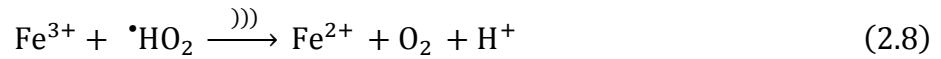
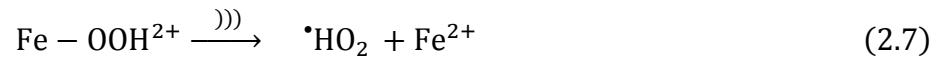
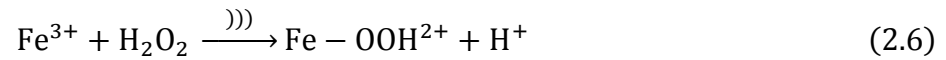
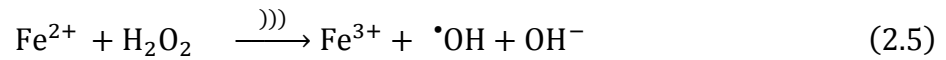
### **2.3 Effect of chemicals additives on the ultrasonic reaction**

The hydroxyl radicals generated by an ultrasonic process could take place in three different regions inside the solution i.e. the gas phase, interface of the cavitation bubbles and the bulk liquid phase. The generation of  $\cdot\text{OH}$  radicals by the sonolysis process alone could be insufficient to degrade organic compounds in addition to the problems of the short life time of these radicals. Therefore, there is a need to add chemical additives having the ability to generate more hydroxyl radicals to assist the radicals formed by ultrasonic process so that the radicals formed during the process can be increased. These additives may either be soluble i.e. Fenton/Fenton-like reagents, NaCl and carbon tetrachloride ( $\text{CCl}_4$ ) (Güyer and Ince, 2011) or gases such as ozonation. The enhancement in the degradation of rhodamine B dye by the addition of NaCl into the sonolysis process has been reported by Behnajady *et al.* (2008). NaCl addition serves to reduce the vapor pressure inside the cavitation bubbles thus, increasing the collapsing rate between these radicals so that more radicals will be formed.

Gogate and Katekhaye (2012) reported the effect of adding different types of additive such as NaCl or radicals promoters i.e.  $\text{H}_2\text{O}_2$  and  $\text{CCl}_4$  into ultrasonic reaction to enhance the efficiency of the process. The results found that the effect of these additives is strongly depends of the reactor operating condition such as intensity and frequency of irradiation which control the inherent cavitational activity.

$\text{CCl}_4$  is a hydrophobic soluble and high volatility additive used in a sonolysis process due to its rapid diffusion into the gas bubbles interface (vapor pressure = 91 mm Hg at 20 °C) that can easily decompose. The enhancement in the activity of the sonolysis process by the addition of  $\text{CCl}_4$  is ascribed to the production of different types of oxidizing agent such as the HOCl and chlorine - containing radicals. Furthermore,  $\text{CCl}_4$  can react with hydrogen atoms to reduce the probability of the  $\cdot\text{OH}$  radicals combination (Gültekin *et al.*, 2009). The removal of phenol using  $\text{CCl}_4$  combined with ultrasonic reaction have been reported by Mahamuni and Pandit (2006). The results showed that the addition of  $\text{CCl}_4$  enhanced the removal of phenol due to the generation of  $\text{Cl}\cdot$  radicals. Both  $\text{H}_2\text{O}$  and  $\text{CCl}_4$  can exist inside the cavitation bubbles. However, the bond energy of C-Cl is lower than that of H-OH bond so that it can be broken more easily. Thus, more  $\text{Cl}\cdot$  radicals are formed to attack organic pollutant in water and convert them into intermediate products. After the formation of these products, the concentration of  $\text{CCl}_4$  will be reduced to allow more  $\text{H}_2\text{O}$  to enter the cavitation bubbles so that more  $\cdot\text{OH}$  radicals will be generated. As a result, both radicals will enhance the sonolysis process leading to the enhancement in the removal of organic pollutant in the water.

The addition of  $\text{Fe}^{2+}$  or  $\text{Fe}^{3+}$  combined with  $\text{H}_2\text{O}_2$  and the ultrasonic process is one the most efficient processes that have been used in wastewater treatment. As it is well-known, the addition of the  $\text{Fe}^{2+}/\text{H}_2\text{O}_2$  is called the Fenton reaction while the combination  $\text{Fe}^{3+}$  and  $\text{H}_2\text{O}_2$  is known as the Fenton-like reaction ( $\text{Fe}^{3+}/\text{H}_2\text{O}_2$ ). Both the Fenton and Fenton-like reactions can occur simultaneously and generate the  $\cdot\text{OH}$  radicals (Pang *et al.*, 2011b) as shown in the following equations (Jamalluddin and Abdullah, 2011b).



Despite the high efficiency of homogeneous Fe catalyst, there are some drawbacks in the use of Fe metals alone in an ultrasonic process. The high-cost associated with the consumption of hydrogen peroxide, limited applicable range of positive pH value and separation difficulties of iron ions from the treated solution to hinder the successful use of the Fenton reaction in real applications (Chen *et al.*, 2010).

Tezcanli-Güyer and Ince (2004) reported a comparative study between ultrasonic and ultrasonic-assisted O<sub>3</sub> for the decolorization of acid orange 7. The results revealed that the decolorization by ultrasonic alone was slower ( $k = -21.33 \times 10^{-3} \text{ min}^{-1}$ ) than that after addition of O<sub>3</sub> ( $k = -79.45 \times 10^{-3} \text{ min}^{-1}$ ). The acceleration of the decolorization efficiency of the process due to the higher mass transfer of ozone with the mechanical stirring provided by ultrasonic leading to increase the  $\cdot\text{OH}$  generation during the reaction. However, an optimum amount of addition should be put in mind to reduce the cost of the process.

Many successful research works have been done in the field of wastewater treatment by combining the use of additives with ultrasound. However, these additives may not be effective in all the cases as there will an optimum level for its

used and the formation of some toxic by-products with the use of these additives. In addition, the cost of the use of these additives in huge amounts in the real industrial wastewater treatments makes this process unfavorable. Therefore, there is a need to create an effective solution that can be practically used in industry while at the same time being cost-effective.

#### **2.4 Combination of ultrasound with other processes**

In order to enhance the efficiency of the ultrasonic process, different reports have been published on the synergic effect between ultrasound and other processes i.e. with photocatalyst (Naomi *et al.*, 2000), ozone (Sancar and Balci, 2013) and Fe reagent (Zhang *et al.*, 2005). The authors found that the combination of ultrasound with other processes enhance the degradation of organic compound and reduced the time needed to run the process. Besides, the ultrasound has the ability to clean the surface of the catalyst. Agitation can improve the mass transfer of reactants and products to and from the catalyst surface. Table 2.1 present some reports about the ultrasonic process combined with other process for the degradation of organic dyes.

**Table 2.1.** The ultrasonic process combined with other advanced oxidation processes

Pollutant	Process		Important finding	Refrencess
Acid black 1	US+Fenton	i)	The degradation efficiency of AB1 increased with the increasing ultrasonic level.	Sun <i>et al.</i> (2007a)
		ii)	Oxidation power of low concentration of iron in Fenton reaction could be significantly enhanced by the US.	
Rhodamine B	US+ Electrocatalytic	i)	US irradiation can eliminate the impurity layers at the surface of electrode, increasing applied potential electrode thus, increased its activity.	Ai <i>et al.</i> (2010)
		ii)	Obvious synergistic effect in the US–EO process compared to either ultrasound (US) process or electrocatalytic oxidation (EO) process.	
Red X-GRL	Sono-Electro Fenton	i)	US increased the production of H <sub>2</sub> O <sub>2</sub>	Li <i>et al.</i> (2010a)
		ii)	Sono-Electro Fenton enhanced the decolorization of the dyes compared to the Electro-Fenton.	
Methyl orange	US+UV+TiO <sub>2</sub>	i)	The sonophotocatalytic system showed an increase in degradation rate compared to sonocatalytic or photocatalytic system.	Cheng <i>et al.</i> (2012)
		ii)	All the operation parameters such as TiO <sub>2</sub> dosage, US power, air fow and liquid circulation velocity showed optimal values and such increase cause reduction in the efficieny of the process.	

## 2.5 Sonocatalytic reaction

The synergic between heterogeneous catalysts and ultrasonic process has received a great attention in the last decade due to the high catalytic activity in the production of more hydroxyl radicals to enhance the efficiency of the degradation process. The use of ultrasound as an irradiation source for the heterogeneous catalysts can be useful in many aspects such as, improvement in the diffusion of reactant from the bulk solution to the surface of catalyst, enhancement in the chemical reaction on the surface of the catalyst due to the presence of the  $\cdot\text{OH}$  radicals on its surface and continuous cleaning of the catalyst surface which is ascribed to the desorption of the generated product during oscillation. In addition, ultrasonic process prevents the aggregation of the catalyst particles due to the fragmentation of the particles into smaller sizes thus increasing the active surface area available for the reaction (Pang *et al.*, 2011b). The addition of heterogeneous semiconductor catalysts such as  $\text{TiO}_2$  seems to be an efficient method for enhancing the degradation of organic pollutants by increasing the formation of  $\cdot\text{OH}$  radicals in this system (Shimizu *et al.*, 2008).

Titanium oxide is one of the most important heterogeneous catalysts in photocatalytic reactions. It is due to its non-toxic property, inexpensive and highly reactive nature under UV irradiation that has been widely adopted to oxidize organics in wastewater (Huang *et al.*, 2008) as well as its high durability, corrosion resistance, and high oxidation potential (Yamaguchi *et al.*, 2010). Sonocatalytic process could enhance the generation of radicals with the use of an active catalyst that has the ability to provide additional nuclei and increases the decomposition of  $\text{H}_2\text{O}$ . Thus, more radicals will be formed to enhance the efficiency of the process (Jamalluddin and Abdullah, 2011a) as in the following equations:



Abdullah and Ling (2010) offered an explanation on the effect of heat treatment on the sonocatalytic activity of TiO<sub>2</sub> using different types of dye such as congo red, methyl orange, and methylene blue. The authors concluded that the activity of the catalyst depended on the composition and phase change of the TiO<sub>2</sub> in addition to the chemical structure and molecular weight of the dye molecules. The highest removal efficiency was obtained with congo red of an initial concentration of 10 mg/L, 1.5 g/L of catalyst loading and 450 mg/L of H<sub>2</sub>O<sub>2</sub>.

It is well known that bare TiO<sub>2</sub> has a small surface area compared to other types of heterogeneous catalysts. Many successful research works have been carried out to increase the surface area of TiO<sub>2</sub> by converting it to nano tube TiO<sub>2</sub> (Pang and Abdullah, 2011) and nano particles TiO<sub>2</sub> (Abbasi and Asl, 2008). Wang *et al.* (2006c) have been conducted a comparison study for the degradation of methyl parathion using both powder and nanometer anatase titanium oxide. The results indicated that the sonocatalytic activity of nanometer anatase TiO<sub>2</sub> was better than that of ordinary anatase TiO<sub>2</sub> powder due to the small particles size and higher surface area. The maximum degradation efficiency of methyl parathion by the nanometer anatase was about 90 % within 50 min at an optimum conditions of 50 mg/L initial concentration

of methyl parathion, 1000 mg/L amount of catalyst, ultrasonic frequency of 40 kHz, output power of 50 W and pH value 10.0.

Several other research works have been also conducted to study the use of the sonocatalytic reaction for the degradation of various types of dyes. Wang *et al.* (2007b); Wang *et al.* (2008c) and Wang *et al.* (2011b) all concluded that the modified TiO<sub>2</sub> showed better catalytic activity than the commercial TiO<sub>2</sub>. The enhancement in the sonocatalytic activity was ascribed to the higher surface area and the generation of more active radicals during the reaction. These radicals are formed from the excitation of the titanium oxide by the absorbance of the UV light generated from the ultrasonication. In addition, to the sonolysis of water, more radicals that are formed will lead to higher degradation efficiency.

## **2.6 Zeolite as a molecular sieve support**

Recently, molecular sieves such as zeolite have received a great attention owing to their unique structures and special properties that make them suitable to be used in multiple industrial processes. Zeolite are crystalline aluminosilicates having a regular structure of SiO<sub>4</sub> and AlO<sub>4</sub> connected into 3-diamantional framework which are responsible for the formation of pores and cavities network in the zeolite structure (Kaduk and Faber, 1995). The ability of zeolite to act as a guest host for many heteroatom's in addition to different metals is ascribed to the presence of these pores and cages with an opining size range from 4-14 Å (Chatti *et al.*, 2007).



These special properties of zeolites in addition to their high surface area, high thermal stability, eco-friendly and their ability for accepting or donating electrons increase their advantages compared to other supports (Ökte and Yilmaz, 2009a). The main structure of zeolite consists of neutral tetrahedral network of  $\text{SiO}_4$  and negative network  $\text{AlO}_4^-$ . The negative charges of  $\text{AlO}_4^-$  are balanced by cations at the extraframework such as alkali metals or quaternary ammonium ions. The number of Al content determines the number of exchangeable cations. Thus, the Al (Si/Al ratio) content affects the thermal and chemical stability or the polarity of the internal surfaces (Garcia and Roth, 2002). In addition, the Si/Al ration can also affect the hydrophilic / hydrophobic properties of the zeolite by changing its adsorption ability especially when the zeolite are used as supports for metals (Najar *et al.*, 2010).

The zeolite Y is a faujasite molecular sieve with a main structure of sodalities cages. These super cavities or sodalities cages with a diameter of 13 Å form their structure from the interconnected tetrahedral of the smaller pores with an opening diameter of 7.4 Å (Taufiqurrahmi *et al.*, 2011). The main chemical structure of zeolite can be expressed as

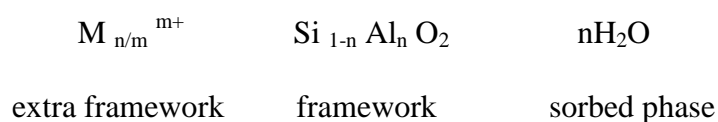
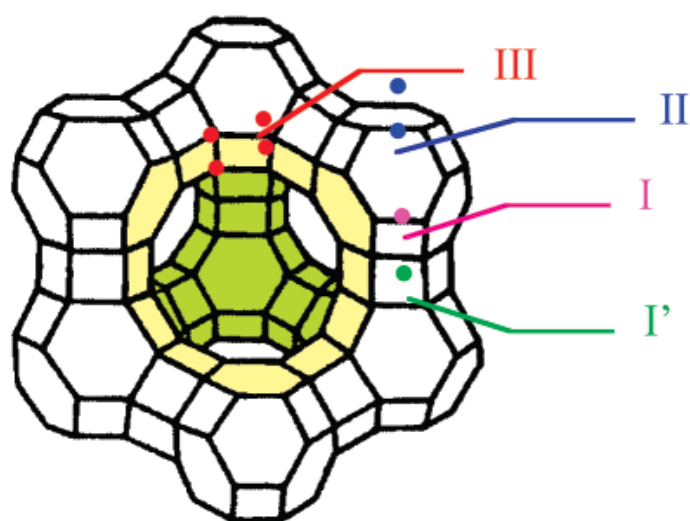


Figure 2.3 presents the postulated sites of the cations for extra framework of cations-exchanged faujasites where I is in the sodalite cage, adjacent to a hexagonal ring shared by the sodalite cage and a double 6-ring, II is in the sodalite cage, adjacent to an unshared hexagonal face, III is at the super cages and I' is at the center of the double 6-rings.



**Figure 2.3** Faujasite supercavities (R-cages) constructed of sodalite cages and hexagonal prism subunits with the charge compensating cations occupying different crystallographic positions are designated by Roman numerals (Garcia and Roth, 2002).

### 2.6.1 TiO<sub>2</sub> loaded on different supports

Several studies have been reported on the degradation of organic dyes using suspensions of TiO<sub>2</sub> powder in the polluted solution. However, there are several limitations to use 'bare' TiO<sub>2</sub> due to the fact of its rapid aggregation in suspension, resulting in smaller effective surface area and lower catalytic efficiency. The small size of TiO<sub>2</sub> particles complicates the filtration of suspensions during the process. Moreover, owing to TiO<sub>2</sub> polar surface, the pollutant-adsorbing ability of TiO<sub>2</sub> often appears to be low especially for non-polar, organic compounds (Wang *et al.*, 2008a).

Supporting TiO<sub>2</sub> on different porous materials is a plausible solution to eliminate the drawbacks of using bare TiO<sub>2</sub>. Many important considerations have to be kept in mind when choosing a good support to anchor TiO<sub>2</sub> such as the surface characteristics, stability of the material, hydrophilic/hydrophobic properties, etc. In